

# Effect of Fe<sub>2</sub>O<sub>3</sub> Nano Filler on Structural and Electrical Properties of PVB-NaNO<sub>3</sub> Complexed Solid Polymer Electrolytes for Electrochemical Cell Applications

Umadevi Prasanna<sup>1</sup>, Vijaya Kumar Kambila<sup>1,1</sup>, Krishna Jyothi Nadella<sup>2</sup>

<sup>a</sup>Department of Physics, Dayananda Sagar University, Harohalli, Ramanagara Dt, Bengaluru 562112, India

<sup>b</sup>Department of Physics, Satya Sai University of Human Excellence, Kalburgi, Karnataka, India

## Abstract

The composite solid polymer electrolyte films were prepared by doping nano-sized Fe<sub>2</sub>O<sub>3</sub> particles on PVB (Polyvinyl Butyral) complexed with NaNO<sub>3</sub> salt by solution casting technique. FTIR, XRD, and SEM methods characterized these electrolyte films. The Fourier Transform Infrared Spectroscopy and X-ray diffraction techniques reveal the structural and complexation changes occurring in the electrolytes. The surface morphology of the electrolyte film was examined using the SEM (Scanning Electron Microscope) technique. The PVB+NaNO<sub>3</sub>+Fe<sub>2</sub>O<sub>3</sub>(70:30:3%) electrolyte shows a moderate ionic conductivity of  $2.51 \times 10^{-5} \text{ S cm}^{-1}$  at ambient temperature (303 K). AC impedance spectroscopic analysis evaluates the ionic conductivity of the produced polymer electrolyte. Wagner's polarisation technique was applied to study the charge transport characteristics in the electrolyte films. The investigation revealed that ions constituted the majority of the transport carriers. An Open Circuit Voltage (OCV) of 2.0V and a Short Circuit Current (SCC) of 0.8 mA were found in the discharge characteristics data for the cell constructed with the polymer electrolyte sample.

---

**Keywords:** Polymer electrolytes, X-ray diffraction, Ionic conductivity, Discharge characteristics, Optical properties, Transference number.

---

1 Corresponding author. Tel.: +91-900-059-7487;  
E-mail address: drkambilavk@gmail.com

## 1. Introduction

Solid electrolytes have many advantages over liquid electrolytes, including better ionic conductivity, greater mechanical strength, good chemical and thermal stability, and better compatibility with electrode materials. These advantages can be applied to various devices, including fuel cells, electrochemical devices, electrochromic panels, and supercapacitors [1-5]. Therefore, many investigations are being done worldwide on solid polymer electrolytes to improve conductivity by chemically modifying the surface morphology of the electrolyte. This modification improves by forming a low resistivity layer at the electrolyte-electrode interface. However, the cost of these polymer electrolytes with changed surfaces is high. Consequently, composite polymer films with several components that are loaded with salts and alcohols are being used as a starting material for studies [6-8]. It changes the physicochemical characteristics of the blended films, increasing the conductivity compared to all other inorganic compounds.

In this work, a PVB-based solid polymeric electrolyte was prepared by using PVB as the host polymer. Polyvinyl butyral, or PVB, is a translucent, strong, and flexible thermoplastic substance. It also adheres well to a wide range of substrates and has excellent optical clarity. It is made mostly of polyvinyl alcohol by a chemical reaction involving formaldehyde and butyraldehyde. The resin's exceptional UV resistance and film-forming capacity are widely known. The cheap and easily accessible polymer polyvinyl butyral, or PVB, is made from polyvinyl alcohol, or PVA. When polyvinyl alcohol and butyraldehyde combine in an acidic environment, it is produced. There is no clear crystallinity and the resultant copolymer is random. Because it contains hydrophilic hydroxyl groups, hydrophobic butyral groups, and tiny acetyl moieties, PVB can be combined with hydrophilic and hydrophobic components. Polymer hydrophilicity or hydrophobicity can be adjusted by varying the monomer composition [9]. Despite being widely utilized in automotive safety glasses as an interlayer material to increase durability and reduce the effects of ultraviolet light, PVB also possesses the intriguing ability to form complexes with both inorganic and organic salts. These PVB-salt complexes maintain the amorphous form of the host polymer, thereby overcoming crystallization-related problems that significantly affect ionic mobility and the overall effectiveness of solid polymer electrolytes (SPEs) [10]. Despite a wealth of literature on the subject, there has been little focus on using PVB as a host polymer. Thin-film polymeric electrolytes based on photovoltaic beads (PVBs) have been employed in several studies to enable dye-sensitized solar cells [11]. The Morphology and Thermal Degradation Kinetics of Poly (vinyl butyral) Cast Films Made with Various Organic Solvents [12]. Polyvinyl butyral-Al (NO<sub>3</sub>)<sub>3</sub> composite solvent production and characterization for alumina-based fiber [13]. Sodium is another material abundantly available on earth which is a non-toxic material and has a very high electrochemical potential. Hence sodium can be used in electrolyte preparation and battery applications.[14]. Recent research has focused on sodium ion conducting systems for their possible application in solid-state batteries with high cell voltages and energy densities since sodium metal ions are readily available and inexpensive. Few efforts have been made to use sodium ion complexes to raise the sodium ion conductivity.

Hematites (Fe<sub>2</sub>O<sub>3</sub>) is a mineral widely available on earth and belongs to the iron-oxide minerals group. They have a paramagnetic behavior and have a hexagonal structure. As Hematites are environment friendly [15], the cheapest semiconductor material [16-17], and show strong catalytic activity, they become more suitable to be used in battery applications. Because the material can absorb visible light and retain up to 45% of solar spectrum energy, it can also be used in visible light photocatalysis. Nanoparticles can be composed with PVB-based films to improve conductivity and the mobility of ions and electrons. Moreover, composition stabilizes the films [18]. The improved conductivity of the nanoparticle-composed films is a result of the decreased surface area/volume ratio and other morphological changes associated with the nanoparticles. Different investigation reports and literature survey shows the composition of nano-ZnO and ceramic nanofillers in PVB films to improve the electrical properties. [19-20]. The purpose of this study is to produce and evaluate nano-Fe<sub>2</sub>O<sub>3</sub>-

composed PVB + Sodium Nitrate composite films using XRD, SEM, FTIR, and AC impedance spectroscopy, and to investigate their potential use in the construction of electrochemical cells.

## 2. Experimental

### 2.1 Materials and preparation of the polymer electrolyte films

KF Chemicals supplied the sodium nitrate ( $\text{NaNO}_3$ ), methanol, and polyvinyl butyral (PVB). Sigma Aldrich provides the nanofiller,  $\text{Fe}_2\text{O}_3$ . None of the chemicals were refined or altered before usage. The solution casting method was used to generate the necessary concentration of PVB and  $\text{NaNO}_3$  in a 70:30 ratio, and nanofiller- $\text{Fe}_2\text{O}_3$  was added in compositions of 1%, 2%, and 3%. During the preparation, methanol was utilized as the solvent. After combining the necessary amounts of PVB,  $\text{NaNO}_3$  salt, and nanofiller  $\text{Fe}_2\text{O}_3$ , the resultant mixture was constantly stirred at room temperature for 48 hours to create a clear, uniform solution. In a vacuum chamber, this solution was allowed to dry in the polypropylene dishes at ambient temperature. The methanol in the homogenous mixture progressively evaporated at that temperature under vacuum drying. A somewhat translucent film developed after 24 hours. Following the experiments, the polymer electrolyte film was taken out of the dishes and put in a vacuum desiccator.

### 2.2 Materials Characterization

An X'pert diffractometer was used to examine the produced films' XRD pattern. With the  $\text{CuK}\alpha$  radiation of  $\lambda = 1.5403 \text{ \AA}$ , the diffraction factors for the films were measured between  $10^\circ$  and  $90^\circ$  of  $2\theta$  values. FTIR (Mid Infrared) Spectrometer-SHIMADZU (Model-206-31010-58) was used to perform Fourier transform infrared (FTIR) spectroscopy. Using a  $2 \text{ cm}^{-1}$  spectral resolution setting, the measurement was conducted for the  $500\text{--}4000 \text{ cm}^{-1}$  wavenumber range. Using blocking stainless steel electrodes at frequencies between 20 Hz and 2 MHz, the HIOKI 3532-50 LCR meter was employed to examine electric characteristics throughout a temperature range of 303–373 K. At room temperature (303 K), disc-shaped samples were placed between stainless steel electrodes and Wagner's polarization technique was applied. The polarization current as a function of time was measured in response to a 1.5 V DC bias. The plot of polarization current vs. time was used to calculate the ionic transport ( $t_{\text{ion}}$ ) and electronic transport ( $t_{\text{ele}}$ ) quantities. MIRA 3 (FESEM) was used to capture the pictures from the scanning electron microscope (SEM). The most conductive film's discharge properties were investigated.

## 3. Results and Discussion

### 3.1. X-ray diffraction Studies

For the electrolyte film samples with different compositions, XRD measurements were made. The XRD results for different films are displayed in Fig 1. Broad, distinctive peaks have been seen in pure PVB at  $20.82^\circ$ . This peak is expanded and shifted to  $19.35^\circ$  with a decrease in intensity upon the addition of 30% of  $\text{NaNO}_3$  salt [21]. The peak is shifted to  $19.32^\circ$  for 1.0%,  $19.30^\circ$  for 2.0%, and  $19.25^\circ$  for 3.0% when nano- $\text{Fe}_2\text{O}_3$  is present in the 70PVB+30  $\text{NaNO}_3$ (70:30) film. This transition happens as the intensity decreases and the widening increases. It is important to notice that the shift is maximal and well-broadened at 3.0%, without the characteristic strong and abrupt peaks of  $\text{Fe}_2\text{O}_3$ ,  $\text{NaNO}_3$ , or both, and with less intensity. Additionally, the peaks' broadening signifies the formation of a larger amorphous area in the film, which promotes ionic mobility [22]. These alterations in the XRD spectrum show that the components of the film are evenly distributed throughout and that the film with the 3% nano- $\text{Fe}_2\text{O}_3$  has more homogeneous and amorphous sections, indicating its suitability for conductivity studies.

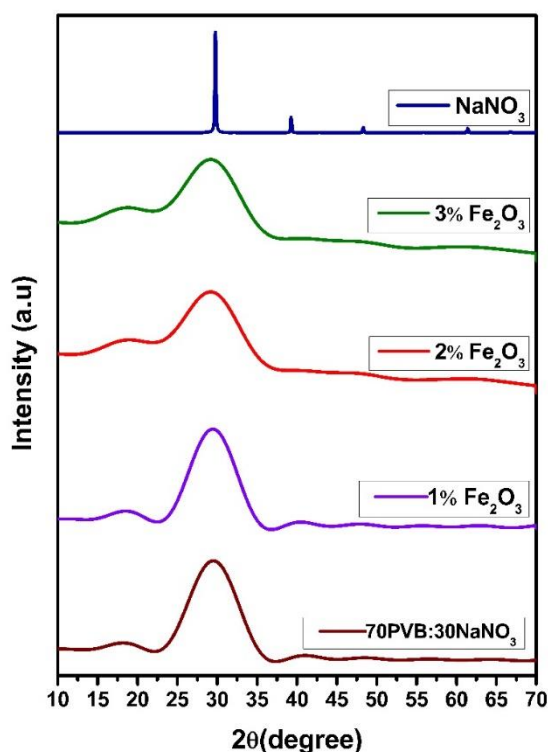


Fig 1: XRD pattern of PVB + NaNO<sub>3</sub>(70:30) and PVB (70%) +NaNO<sub>3</sub>(30%) + nano-Fe<sub>2</sub>O<sub>3</sub> (1–4%) complexed electrolytes and pure NaNO<sub>3</sub> salt.

### 3.2. Fourier transform infrared spectroscopy (FTIR) studies

To understand the complex formation between polymers, salt, and nanofiller, FTIR analysis was done. Fig 2 shows the FTIR data for the polymer electrolyte film with different compositions of nanofiller Fe<sub>2</sub>O<sub>3</sub> added into 70% PVB and 30% NaNO<sub>3</sub>. The measurement data is shown for the wavenumber ranging from 500 to 4000cm<sup>-1</sup>. We observe that the characteristic peak at 3417 cm<sup>-1</sup> is observed for 70PVB:30NaNO<sub>3</sub> combination and this corresponds to the stretching of the Hydroxyl group (O-H). The peaks 2935 cm<sup>-1</sup> and 2870 cm<sup>-1</sup> shown are of the vibrational bands for the 70PVB:30NaNO<sub>3</sub> composition. These peaks belong to the Asymmetric stretching of CH<sub>2</sub> and Symmetric stretching of CH<sub>3</sub> for this polymer [23]. The intensity of the broad peaks was decreased in the addition of nanofillers to the polymeric substance. Likewise, the bands for 70PVB:30NaNO<sub>3</sub> at 1648 cm<sup>-1</sup>, 1377 cm<sup>-1</sup>, and 1066 cm<sup>-1</sup> can be assigned to C=O stretching C-H bending and C-O stretching respectively. When nanofillers are added to a polymeric substance, the intensity of these peaks decreases and their peaks broaden, indicating that complexation between the composed nanofiller Fe<sub>2</sub>O<sub>3</sub> and the host polymer matrix has occurred [24]. However, we also observe that with the addition of nanofiller Fe<sub>2</sub>O<sub>3</sub> into the polymer matrix of PVB-NaNO<sub>3</sub>, there are new peaks observed at 2394cm<sup>-1</sup> and 1771cm<sup>-1</sup> in the nanocomposite films of PVN+NaNO<sub>3</sub>+Fe<sub>2</sub>O<sub>3</sub>.

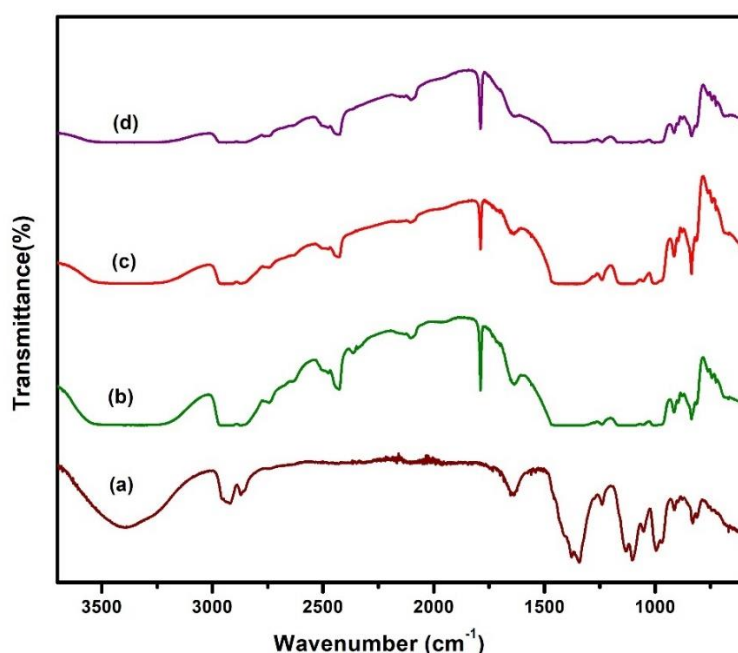


Fig 2. FTIR analysis spectra of PVB+NaNO<sub>3</sub>+Fe<sub>2</sub>O<sub>3</sub> polymer electrolyte films. (a) 70PVB+30NaNO<sub>3</sub>, (b) 1% Fe<sub>2</sub>O<sub>3</sub>, (c) 2% Fe<sub>2</sub>O<sub>3</sub>, (d) 3% Fe<sub>2</sub>O<sub>3</sub>.

### 3.3.SEM Analysis

The study on the surface morphology of the polymer electrolytes was done using Scanning Electron Microscopy (SEM). Fig 3 (a-d) shows the images of the SEM study for 70PVB:30NaNO<sub>3</sub> and 70PVB:30NaNO<sub>3</sub>:(1-3wt%) Fe<sub>2</sub>O<sub>3</sub> nanocomposite polymer electrolyte films with different magnifications. It can be observed from the images that there is a significant variation in the surface morphology in the complex polymer matrix which is added with nano Fe<sub>2</sub>O<sub>3</sub> filler. The absence of roughness suggests that the host polymer electrolyte films have dissolved the nanofillers Fe<sub>2</sub>O<sub>3</sub>. X-ray diffraction measurements corroborated the appearance of a more amorphous composite film with 3 weight percent Fe<sub>2</sub>O<sub>3</sub> distributed nanoparticles when compared to other compositions. The smooth and homogenous surface morphology of the 70PVB:30NaNO<sub>3</sub> and 1-3 weight percent Fe<sub>2</sub>O<sub>3</sub> complexed polymer electrolyte film suggests its amorphous nature [25]. Lumps of Fe<sub>2</sub>O<sub>3</sub> are seen on the membrane surface and a crystalline structure contained in the polymer matrix is visible in the surface morphology of the nanocomposite polymer films [26]. The amorphous character of the host polymer electrolyte is reflected in the background's darkness and smoothness. It suggests an amorphous nature, which is consistent with the XRD findings.

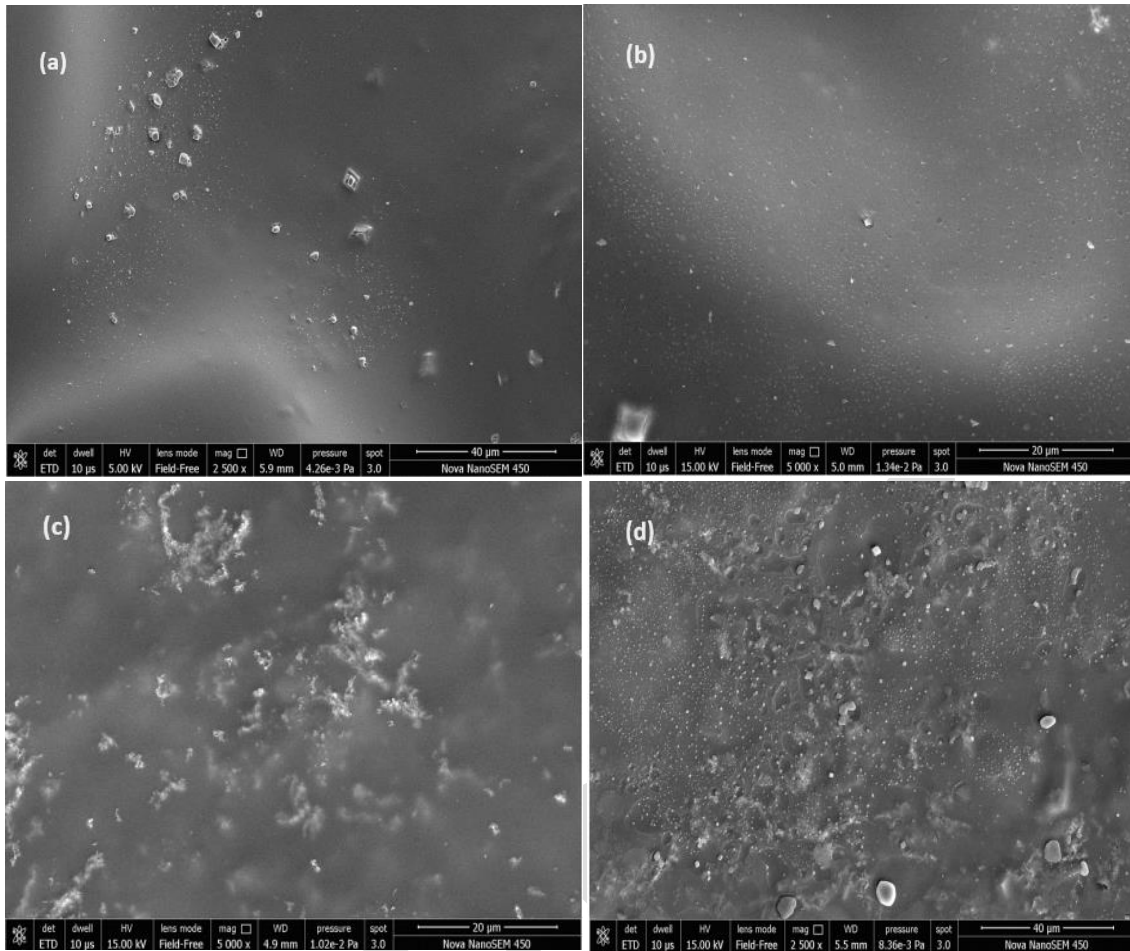


Fig 3. SEM images of PVB+NaNO<sub>3</sub>+Fe<sub>2</sub>O<sub>3</sub> polymer electrolyte films. (a) 70PVB+30NaNO<sub>3</sub>, (b) 1% Fe<sub>2</sub>O<sub>3</sub>, (c) 2% Fe<sub>2</sub>O<sub>3</sub>, (d) 3% Fe<sub>2</sub>O<sub>3</sub>.

### 3.4. Transference Number measurements

The electrolyte films were subjected to Wagner's polarization technique to find out the transference numbers. These numbers are significant in classifying the polymer electrolyte films. For this measurement, the system was constructed with the combination Ag/PVB+NaNO<sub>3</sub>+Fe<sub>2</sub>O<sub>3</sub>/Ag and polarized at 303K by supplying a constant supply voltage of 1.5V. We were able to evaluate how much ions and electrons contributed to the films' conductivity using this method. We used the below equations.

$$t_{ion} = 1 - I_f/I_i \quad (1)$$

$$t_{ele} = I_f/I_i \quad (2)$$

Where the initial current is denoted by  $I_i$  and the final current by  $I_f$ . The calculation showed the transference numbers for ions were 0.98-0.997. The data is shown in Fig 4 and Table 1. We observe from Table 1 that, the maximum contribution for charge carriers is from ions and the contribution from electrons is minimal. Also, we observe that the film with a composition of 3.0% Fe<sub>2</sub>O<sub>3</sub> has higher conductivity and lower activation energy and crystallinity. The transference numbers for ions in the films tend towards unity, which shows that these polymer electrolyte films are suitable for building solid-state electrochemical cells [27-28].

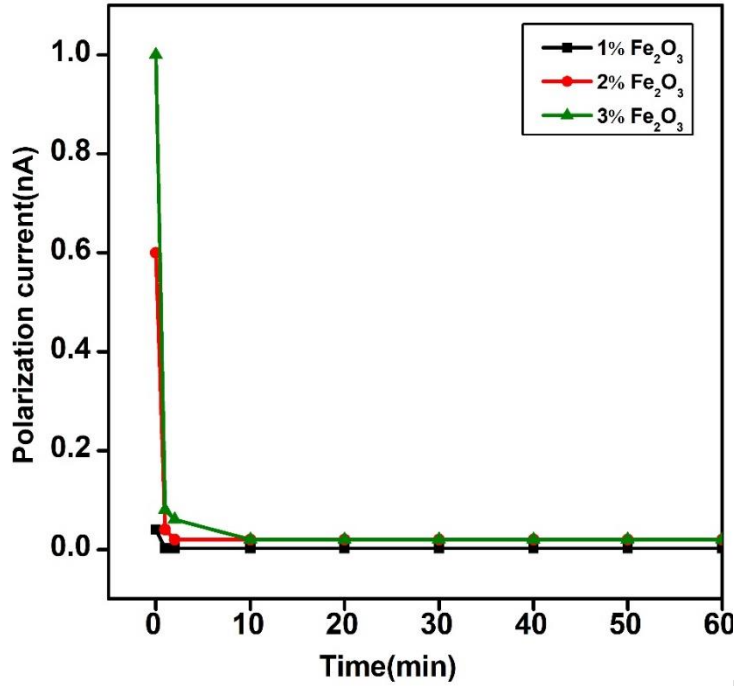


Fig 4. Polarisation current vs time for polymer electrolyte films with varying Fe<sub>2</sub>O<sub>3</sub> weight percentage ratios.

### 3.5. Conductivity Studies

The Conductivity plots for PVB+NaNO<sub>3</sub>+Fe<sub>2</sub>O<sub>3</sub> polymer electrolyte films at room temperature (303 K) for various weight percentage ratios are shown in Fig. 5. A small amount of AC voltage was applied across the sample, and the Cole-Cole graph was generated using the measurement data. The real part (Z') and imaginary part (Z'') in the frequency range of 20Hz–2MHz were measured using the LCR meter HIOKI 3532-50. Because of the excellent contact between the electrode and electrolyte interfaces, we see an electrode polarisation phenomenon. A semi-circular arc appears at high frequency on the Cole-Cole plot, also called the Nyquist plot, whereas a spike forms at low frequency, indicating bulk resistance. Ionic conduction is primarily responsible for the spike that is generated [29–30]. Table 1 displays the computed values for conductivity. The bulk resistance values (R<sub>b</sub>) can be used to compute the AC conductivity using the equation below.

$$\sigma = t/R_b A \quad (3)$$

In this case, "t" denotes the film's thickness, "A" denotes its area, and "R<sub>b</sub>" stands for bulk resistance. According to the impedance spectra, the bulk resistance of the electrolyte films containing 1 to 3 weight percent Fe<sub>2</sub>O<sub>3</sub> decreases, however as the Fe<sub>2</sub>O<sub>3</sub> level increases, the polymer electrolytes' conductivity improves [31–32]. Fig 6 shows Plots of impedance for the R and C circuits in both series and parallel configurations. Fig 7 shows the change in the logarithm of ionic conductivity with inverse temperature for different Fe<sub>2</sub>O<sub>3</sub> concentrations in the PVB+NaNO<sub>3</sub> complex over the 303–373 K temperature range.

The Arrhenius equation is followed by the temperature (T) as a function of  $\sigma$ .

$$\sigma = \sigma_0 \exp(-E_a/kT) \quad (4)$$

Where  $T$  is denoted by absolute temperature, the activation energy is denoted by  $E_a$ , the Boltzmann constant is represented by  $k$ , and the pre-exponential factor is denoted by  $\sigma_0$ . The activation energy values were calculated from the slopes shown in Table 1. The computed values of activation energy fall between 0.18 and 0.35 eV. With an increase in  $\text{Fe}_2\text{O}_3$  concentration, we observe a decrease in activation energy. This might result from the creation of a charge transfer complex in the lattice, which increases electrical conductivity and lattice charges when dopants are added [33]. In contrast to the other samples, the polymer film  $\text{PVB}+\text{NaNO}_3+\text{Fe}_2\text{O}_3(70:30:3\%)$  exhibits the lowest activation energy and the maximum conductivity. The film with 3.0%  $\text{Fe}_2\text{O}_3$  shows higher conductivity, lower activation energy, and lower crystallinity due to: (1) The disruption of the polymer's crystalline structure, leads to more amorphous regions that facilitate ion movement. (2) The formation of efficient ionic pathways and increased  $\text{Na}^+$  ion mobility due to the interaction of  $\text{Fe}_2\text{O}_3$  with the polymer matrix. (3) An optimal concentration of nanoparticles that promotes conductivity without causing agglomeration or blocking ion pathways. These factors work synergistically to enhance the electrochemical properties of the solid polymer electrolyte, making it more suitable for electrochemical cell applications.

Table 1: Ionic conductivity, activation energy, and transference numbers of polymer electrolyte films with varying PVB +  $\text{NaNO}_3$  + nano- $\text{Fe}_2\text{O}_3$  compositions.

| Polymer electrolytes                                  | Conductivity ( $\text{S cm}^{-1}$ )<br>303 K | Activation<br>energy(eV) | Transference<br>Number |                  |
|---|--|--------------------------|------------------------|------------------|
|   |  |                          | $t_{\text{ion}}$       | $t_{\text{ele}}$ |
| PVB+ $\text{NaNO}_3(70:30)$                           | $3.98 \times 10^{-8}$                        | 0.35                     | 0.98                   | 0.012            |
| PVB+ $\text{NaNO}_3+\text{Fe}_2\text{O}_3(70:30:1\%)$ | $1.58 \times 10^{-6}$                        | 0.30                     | 0.991                  | 0.009            |
| PVB+ $\text{NaNO}_3+\text{Fe}_2\text{O}_3(70:30:2\%)$ | $4.46 \times 10^{-6}$                        | 0.25                     | 0.995                  | 0.005            |
| PVB+ $\text{NaNO}_3+\text{Fe}_2\text{O}_3(70:30:3\%)$ | $2.51 \times 10^{-5}$                        | 0.18                     | 0.997                  | 0.003            |

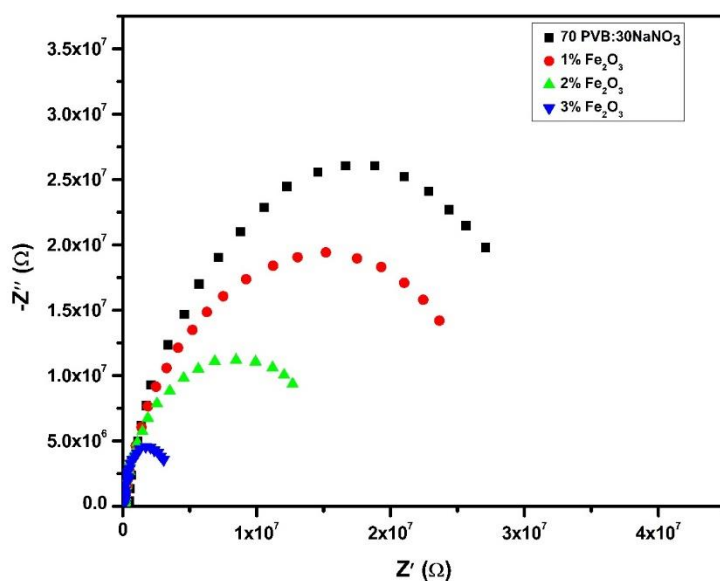




Fig 5: Cole-Cole plots for the PVB: NaNO<sub>3</sub>+Fe<sub>2</sub>O<sub>3</sub> polymer electrolyte films for varying weight percentages at 303K

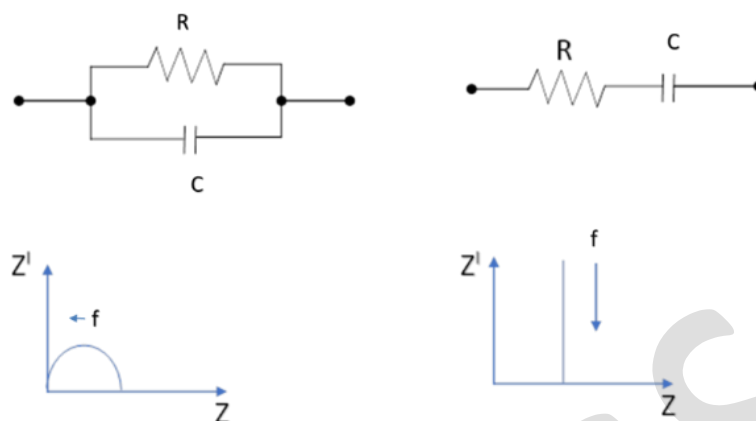


Fig 6: Plots of impedance for the R and C circuit in both series and parallel configurations

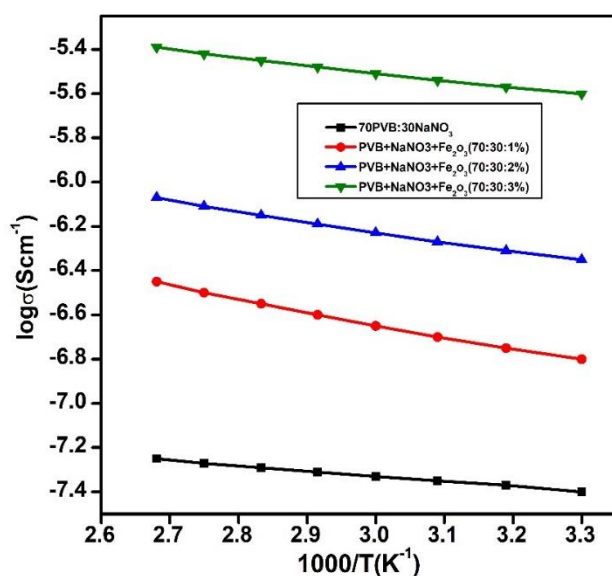


Fig 7. Plots of  $\log \sigma$  vs  $1000/T$  for 70PVB+30 NaNO<sub>3</sub> and PVB+NaNO<sub>3</sub>+Fe<sub>2</sub>O<sub>3</sub> at various weight percent ratios.

### 3.6. Discharge characteristics

Solid-state batteries are made using polymer electrolyte films based on polyvinyl butyral complexed with nano-Fe<sub>2</sub>O<sub>3</sub> and sodium nitrate salt. The following arrangements were utilized to produce solid-state electrochemical cells at room temperature: Cathode: (I<sub>2</sub> + C + electrolyte) / (70PVB + 30NaNO<sub>3</sub> + 3% Fe<sub>2</sub>O<sub>3</sub>) / Na (anode) [34]. Fig 8 shows the discharge characteristics of the cell at room temperature and a constant load of 100 kΩ. As a result of the polarisation effect, the voltage first drops dramatically. The most conductive polymer electrolyte system, 70 PVB + 30 NaNO<sub>3</sub> + 3% Fe<sub>2</sub>O<sub>3</sub>, has been evaluated concerning cell properties, including discharge capacity, open circuit voltage (OCV), short circuit current (SCC), current density, power density, and energy density. In Table 2, the outcomes are displayed [35–36].

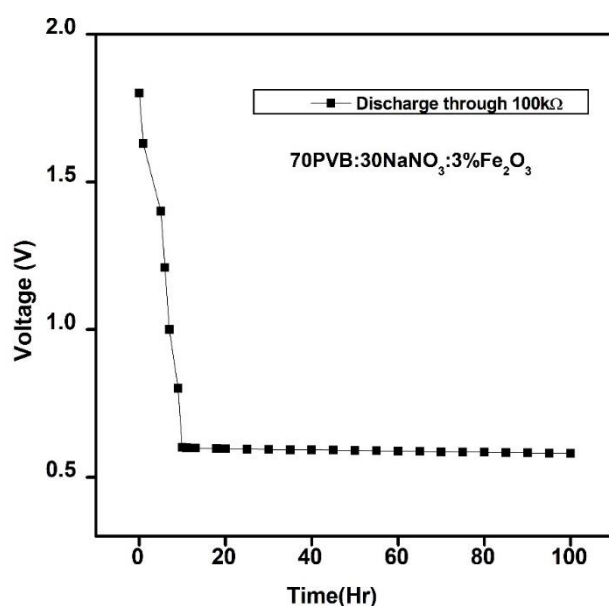


Fig 8. Discharge properties of an electrochemical cell with a 70 PVB + 30 NaNO<sub>3</sub> + 3% Fe<sub>2</sub>O<sub>3</sub> polymer electrolyte (load = 100 kΩ)

Table 2: The electrochemical cell's parameters.

| Cell parameters       | Cell discharge values of<br>70PVB:30NaNO <sub>3</sub> :3%Fe <sub>2</sub> O <sub>3</sub> |
|-----------------------|---|
| Open circuit voltage  | 2.0 V   |
| Short circuit current | 0.8 mA  |
| Area of the cell      | 1.23 cm <sup>2</sup>  |
| Weight of the cell    | 1.2 g   |
| Discharge time        | 100 h   |
| Power density         | 1.3 W Kg <sup>-1</sup>  |
| Energy density        | 130 Wh Kg <sup>-1</sup>   |
| Current density       | 0.65 mA cm <sup>-2</sup>  |
| Discharge capacity    | 80 mA h   |

#### 4. Conclusions

Through the solution casting method, Fe<sub>2</sub>O<sub>3</sub> nanoparticles were composed of PVB (poly vinyl butyral) complexed with NaNO<sub>3</sub> salt to create solid-state ion-conducting polymer electrolyte films. According to XRD, when the concentration of salt increases, the peak's strength decreases. XRD and FTIR investigations verified that the salt and nanofiller had complexed with the polymer. The smooth and homogenous surface morphology of the 70PVB:30NaNO<sub>3</sub> and 1-3 weight percent Fe<sub>2</sub>O<sub>3</sub> complexed polymer electrolyte film suggests its amorphous nature. The conductivity

measurements at room temperature indicate that the maximum conductivity for 70 PVB + 30 NaNO<sub>3</sub> + 3% Fe<sub>2</sub>O<sub>3</sub> is  $2.51 \times 10^{-5}$  S/cm. The ionic and electronic numbers transference is detected within the range of 0.991–0.997. Consequently, the majority of charge carriers in these polymer electrolyte films are ions rather than electrons. The conductivity of the 3.0% Fe<sub>2</sub>O<sub>3</sub>-PVB-NaNO<sub>3</sub> electrolyte is significantly higher than other polymer electrolytes with different nano-fillers, likely due to enhanced ionic mobility in the amorphous phase. The activation energy in this study is lower compared to other studies, highlighting Fe<sub>2</sub>O<sub>3</sub>'s role in facilitating ion transport. The crystallinity reduction is more pronounced in this system, allowing for better ion conduction pathways than in similar polymer-nanofiller systems. Electrochemical stability is expected to be on par or better compared to other systems, though direct comparisons should be made with specific experimental data. This comparative analysis shows that Fe<sub>2</sub>O<sub>3</sub> nanoparticles have a significant positive effect on the ionic and structural properties of the PVB-NaNO<sub>3</sub> electrolyte, outperforming many other systems. A solid-state battery was constructed using these polymer electrolyte films, and the battery's discharge characteristics were investigated.

### Acknowledgments

The management of DSI Bangalore is acknowledged and thanked by Umadevi Prasanna, the author, and Dr. Vijaya Kumar Kambila, the supervisor, for their unwavering support and encouragement. We would like to convey our sincere appreciation for the invaluable assistance provided by Vice Chancellor, Dr. Puttamadappa, Registrar, Dean R&D, Dr. Kousalya, and Dr. K R Udaya Kumar Reddy, Dean SOE of Dayananda Sagar University Harohalli, Ramanagara District.

### References

- [1]. Venkata Subba Rao, C., Ravi, M., Raja, V., Balaji Bhargav, P., Sharma, A.K., and Narasimha Rao, V. V. R., "PVP-based polymer electrolytes for solid-state battery applications." *Iranian Polymer Journal*, 2012, 21, 531–536. <https://doi.org/10.1007/s13726-012-0058-6>
- [2]. Ramya, C.S., Selvasekarapandian, S., Savitha, T., Hirankumar, G., Baskaran, R., Bhuvaneshwari, M.S., and Angelo, P.C., "Conductivity and thermal behavior of proton conducting polymer electrolyte based on poly (N-vinyl pyrrolidone)." *European Polymer Journal*, 2006, 42(10), 2672–2677. <http://dx.doi.org/10.1016/j.eurpolymj.2006.05.020>
- [3]. Smitha, B., Sridhar., S and Khan, A.A., "Chitosan–sodium alginate polyion complexes as fuel cell membranes." *European Polymer Journal*, 2005, 41(8), 1859–1866. <https://doi.org/10.1016/j.eurpolymj.2005.02.018>
- [4]. Srivastava, N., and Chandra, S., "Studies on a new proton conducting polymer system: poly(ethylene succinate)+ NH<sub>4</sub>ClO<sub>4</sub>." *European Polymer Journal*, 2000, 36(2), 421–433. [https://doi.org/10.1016/S0014-3057\(99\)00056-7](https://doi.org/10.1016/S0014-3057(99)00056-7)
- [5]. Pu, H.T., and Wang, D., 2006, "Studies on proton conductivity of polyimide/H<sub>3</sub>PO<sub>4</sub>/imidazole blends." *Electrochimica Acta*, 2006, 51(26), 5612–5617. <https://doi.org/10.1016/j.electacta.2006.02.035>
- [6]. Ramesh Babu, J., Ravindranath, K., and Vijaya Kumar, K., "Preparation and Characterization of Nano-Dy<sub>2</sub>O<sub>3</sub>-Doped PVA + Na<sub>3</sub>C<sub>6</sub>H<sub>5</sub>O<sub>7</sub> Polymer Electrolyte Films for Battery Applications." *Advances in Materials Science and Engineering*, 2018, Article ID: 2080369. <https://doi.org/10.1155/2018/2080369>
- [7]. Kamalova, D.I., Abdrazakova., and Salakh, M.Kh., "Relaxation transitions and compatibility of binary blended PVDF/PVB systems." *Journal Non-Crystalline Solids*, 2021, 571, 121077. <https://doi.org/10.1016/j.jnoncrysol.2021.121077>

- [8]. Omer, R.M., Al-Tikrity, E.T.B., Abed, R.N., Kadhom, M., Jawad, A.H., and Yousif, E., "Electrical Conductivity and Surface Morphology of PVB Films Doped with Different Nanoparticles." *Prog. Color Colorants Coat.*, 2022, 15 (3), 191-202. <http://dx.doi.org/10.30509/PCCC.2021.166839.1120>
- [9]. Bartolotta, A., Marco, G.D., Federico, M., Carini, Jr.G., "Rising the molecular mobility of PolyvinylButyral by plasticizers: Towards energy storage applications." *AAPP.*, 2020, 98, 1825-1242.
- [10]. Zhang, F., Dong, G., Liu J., Liu, J., Ye, S, Diao, X., "Polyvinyl butyral-based gel polymer electrolyte films for solid-state laminated electrochromic devices." *Ionics.*, 2017, 23, 1879–1888.
- [11]. Kuei-Fu, C., Chien-Hung, L., Hsin-Kai, H., Chun-Hung, T., Fu-Rong, C., "Polyvinyl Butyral-Based Thin Film Polymeric Electrolyte for Dye-Sensitized Solar Cell with Long-Term Stability." *Int. J. Electrochem.Sci.* 2013, 8(3), 3524–3539.
- [12]. Motlatle, A.M., Bothloko, O.J., Scriba, M.R, Ojijo, V ., Ray, S.S., "The Thermal Degradation Kinetics and Morphology of Poly (vinyl butyral) Cast Films Prepared Using Different Organic Solvents." *AIP Conference Proceedings.* 2020, 2289(1), 020071.
- [13]. Zhang, Y., Ding, Y., Li, Y., Gao, J., Yang, J., "Synthesis and characterization of polyvinyl butyral–Al (NO<sub>3</sub>)<sub>3</sub> composite sol used for alumina-based fibers." *J Sol-Gel Sci Technol.*, 2009, 49, 385–390.
- [14]. Sreekanth, T., Jaipal Reddy, M., Ramalingaiah, S., and Subba Rao, U.V., "Ion-conducting polymer electrolyte based on poly ethylene oxide / complexed with NaNO<sub>3</sub> salt-application as an electrochemical cell." *Journal of Power Sources.*, 1999, 79(1), 105–110. [https://doi.org/10.1016/S0378-7753\(99\)00051-8](https://doi.org/10.1016/S0378-7753(99)00051-8)
- [15]. M R Joya, M.R., Bar´on-Jaimez, J., and Barba-Ortega, J., "Preparation and characterization of Fe<sub>2</sub>O<sub>3</sub> nanoparticles" *Journal of Physics: Conference Series.*, 2013, 466 012004. <https://doi.org/10.1088/1742-6596/466/1/012004>
- [16]. Senthil, R.A., Theerthagiri, J., and Madhavan, J., "Hematite Fe<sub>2</sub>O<sub>3</sub> nanoparticles incorporated polyvinyl alcohol-based polymer electrolytes for dye-sensitized solar cells," *Materials Science Forum.*, 2015, 832, 72-83. <http://dx.doi.org/10.4028/www.scientific.net/MSF.832.72>
- [17]. Priya, W.L.M., and Suthanthiraraj, S.A., "Electrochemical and FTIR Studies of PVDF-HFP/(CF<sub>3</sub>SO<sub>3</sub>)<sub>2</sub>Zn/Fe<sub>2</sub>O<sub>3</sub> Composite Polymer Electrolytes." *International Journal of Innovative Research in Science & Engineering.*, ISSN: 2347-3207.
- [18]. Kumar, D., and Hashmi, S.A., "Ion transport and ion–filler polymer interaction in poly(methyl methacrylate)-based, sodium ion conducting, gel polymer electrolytes dispersed with silica nanoparticles." *Journal of Power Sources.*, 2010, 195(15), 5101–5108. <https://doi.org/10.1016/j.jpowsour.2010.02.026>
- [19]. Azarian, M.H., and Wootthikanokkhan, J., "Improving electrochemical performance of poly(vinyl butyral)-based electrolyte by reinforcement with a network of ceramic nanofillers." *J Solid State Electrochem.*, 2021, 25, 2687–2697. <https://doi.org/10.1007/s10008-021-05035-4>
- [20]. Harandi, D., and Moradienayat, M., "Multifunctional PVB nanocomposite wood coating by cellulose nanocrystal/ZnO nanofiller: Hydrophobic, water uptake, and UV-resistance properties." *Progress in Organic Coatings.*, 2023, 179, 107546. <https://doi.org/10.1016/j.porgcoat.2023.107546>
- [21]. Prasanna, U., Kambila, V.K., Cheruku, R., Nadella, K.J., Kamma, K.V., and Manju V.V., "Electrical, transport, and optical properties of a novel PVB–NaNO<sub>3</sub> complexed solid polymer electrolyte thin-films for a solid-state battery." *Materials Today Proceedings.*, 2023, 92(2), 711-717. <https://doi.org/10.1016/j.matpr.2023.04.187>
- [22]. Polu, A.R., and Rhee, H.W., "Nanocomposite Solid Polymer Electrolytes Based on Poly(ethylene oxide)/POSS-PEG(n=13.3) Hybrid Nanoparticles for Lithium Ion Batteries." *Journal of Industrial and Engineering Chemistry.*, 2015, 31, 323-329. <http://dx.doi.org/10.1016/j.jiec.2015.07.005>
- [23]. Awadhia, A., and Agrawal, S.L., "Structural, thermal and electrical characterizations of PVA:DMSO: NH<sub>4</sub>SCN gel electrolytes." *Solid State Ion.*, 2007, 178 (13–14), 951–958. <https://doi.org/10.1016/j.ssi.2007.04.001>

- [24]. Kumar, S., Manikandan, V.S., Palai, A.K., Mohanty, S., and Nayak, S.K., 2019, "*Fe<sub>2</sub>O<sub>3</sub> as an efficient filler in PVDF-HFP based polymeric electrolyte for dye-sensitized solar cell application.*" *Solid state Ionics.*, 2019, 332, 10-15. <https://doi.org/10.1016/j.ssi.2019.01.006>.
- [25]. Margani, N.K., and Kumar, V., "*Structural And A.C. Conductivity Studies Of (Pan+Naf) Gel Polymer Electrolyte System With ZrO<sub>2</sub> nano Filler For An Electrochemical Cell Applications.*" *Rasayan Journal of Chemistry.*, 2017, 10(4), pp.1218-1225. <http://dx.doi.org/10.7324/RJC.2017.1041723>
- [26]. Goldshtein, K., Golodnitsky, D., Lereah, Y., L. Burstein, L., and Peled, E., "*Study of polymer electrolytes with grafted Aueg Fe<sub>2</sub>O<sub>3</sub> nanoparticle.*" *International Journal of Hydrogen Energy.*, 2014, 39(6), 2909 -2916. <http://dx.doi.org/10.1016/j.ijhydene.2013.01.170>
- [27]. Mohan, V. M., Bhargav, P. B., Raja, V., Sharma, A. K., and Narasimha Rao, V. V. R., "*Optical and Electrical Properties of Pure and Doped PEO Polymer Electrolyte Films.*" *Soft Materials.*, 2007, 5(1), 33-46. <https://doi.org/10.1080/15394450701405291>
- [28]. Ramya, C. S., Savitha, T., Selvasekarapandian, S., and Hiran Kumar, G., "*Transport mechanism of Cu-ion conducting PVA based solid-polymer electrolyte.*" *Ionics.*, 2005, 11, 436-441. <https://doi.org/10.1007/BF02430262>
- [29]. Devi, C., Gellanki, J., Petterson, H., and Kumar, S., "*High sodium ionic conductivity in PEO/PVP solid polymer electrolytes with InAs nanowire filler.*" *Scientific Reports.*, 2021, 11, 20180 <https://doi.org/10.1038/s41598-021-99663-5>
- [30]. Ojur Dennis, J., Ali, M.K.M., Ibnaouf, K.H., Aldaghri, O., Abdel All, N.F.M., Adam, A.A., Usman, F., Hassan, Y.M., and Abdulkadir, B.A., "*Effect of ZnO Nanofiller on Structural and Electrochemical Performance Improvement of Solid Polymer Electrolytes Based on Polyvinyl Alcohol–Cellulose Acetate–Potassium Carbonate Composites.*" *Molecules.*, 2022, 27, 5528. <https://doi.org/10.3390/molecules27175528>
- [31]. Choudhary, S., Sengwa, R.J., "*Effects of different inorganic nanoparticles on the structural, dielectric and ion transportation properties of polymers blend based nanocomposite solid polymer electrolytes.*" *Electrochimica Acta.*, 2017, 247, 924-941, <http://dx.doi.org/doi:10.1016/j.electacta.2017.07.051>
- [32]. Karunaratne, B.A., Nugera, F.A.E., Dissanayake, M.A.K.L., Senadeera, G.K.R., and Mellander, B.-E., "*Effect of alumina filler on spherulite growth and ionic conductivity of PEO9(LiClO<sub>4</sub>) solid polymer electrolyte.*" *Current Science.*, 2021, 120(5), <https://doi.org/10.18520/cs%2Fv120%2Fi5%2F900-906>
- [33]. Ganesan, R., Dhinasekaran, D., Paramasivam, T., Boukos, N., Vengidusamy, N., and Arumainathan, S., "*Preparation and Characterization of Polyindole–Iron Oxide Composite Polymer Electrolyte Containing LiClO<sub>4</sub>.*" *Polymer-Plastics Technology and Engineering.*, 2012, 51(3), 225–230. <https://doi.org/10.1080/03602559.2011.618159>
- [34]. Basha, S.K.S., Sunita Sundari, G., Vijay Kumar, K., Rao, M.C., "*Structural and Dielectric Properties of PVP Based Composite Polymer Electrolyte Thin Films.*" *J Inorg Organomet Polym.*, 2016, 27(2), 455-466. <https://doi.org/10.1007/s10904-016-0487-3>
- [35]. Venkata Subba Rao, C., Ravi, M., Raja, V., Balaji Bhargav, P., Ashok Kumar Sharma, A., and Narasimha Rao, V.V.R., "*Preparation and characterization of PVP-based polymer electrolytes for solid-state battery applications.*" *Iran Polym J.*, 2012, 21, 531–536. <https://doi.org/10.1007/s13726-012-0058-6>
- [36]. Duraikkan, V., Sultan, A.B., Nallaperumal, N., and Shunmuganarayana, A., "*Structural, thermal and electrical properties of polyvinyl alcohol/poly(vinyl pyrrolidone)–sodium nitrate solid polymer blend electrolyte.*" *Ionics.*, 2018, 24, 139-151. <https://doi.org/10.1007/s11581-017-2169-8>